

Preparation, characterization, and application of activated carbon from low-cost material for the adsorption of tetracycline antibiotic from aqueous solutions

Afshin Takdastan, Amir Hossein Mahvi, Eder C. Lima,
Mohammad Shirmardi, Ali Akbar Babaei, Gholamreza Goudarzi,
Abdolkazem Neisi, Mohammad Heidari Farsani and Mehdi Vosoughi

ABSTRACT

In this study, a new ZnCl₂ impregnated activated carbon (Zn-AC) was prepared from oak charcoals as low-cost material and used as adsorbent for tetracycline (TC) adsorption. The Zn-AC was characterized using Field Emission-Scanning Electron Microscope, Powder X-ray diffraction, and CHNS-O analyses. Specific surface area of the adsorbent was also measured using the BET isotherm model. The TC adsorption onto the Zn-AC was investigated as a function of solution pH, adsorbent dosage, and inorganic cations (Li⁺, K⁺, Mg²⁺, Ca²⁺, Ni²⁺, and Fe³⁺) and anions (HCO₃⁻, NO₃⁻ and SO₄²⁻) that could interfere in the adsorption of TC. The adsorbate solution pH had no considerable effect on TC adsorption. The adsorption of TC onto the adsorbent was relatively fast and reached the equilibrium after about 120 min. The results showed that all studied cations and anions decreased TC adsorption onto the Zn-AC, but this decrease in TC adsorption was strongly significant for Fe³⁺ and Ni²⁺ ions. The general order kinetic model and the Redlich–Peterson isotherm model provided the best fit to the experimental data. The maximum amount of TC adsorbed onto the Zn-AC (Q_{max}) is 282.06 mg g⁻¹ indicating this adsorbent is a good adsorbent for the removal of TC from aqueous solutions.

Key words | activated carbon, adsorption, nonlinear curve fitting, tetracycline

Afshin Takdastan
Ali Akbar Babaei
Gholamreza Goudarzi
Abdolkazem Neisi
Environmental Technologies Research Center
(ETRC),
Ahvaz Jundishapur University of Medical Sciences,
Ahvaz,
Iran

Afshin Takdastan
Mohammad Shirmardi (corresponding author)
Ali Akbar Babaei
Gholamreza Goudarzi
Abdolkazem Neisi
Mehdi Vosoughi
Department of Environmental Health Engineering,
School of Public Health,
Ahvaz Jundishapur University of Medical Sciences,
Ahvaz,
Iran
E-mail: shirmardim@yahoo.com

Amir Hossein Mahvi
Department of Environmental Health Engineering,
School of Public Health,
Tehran University of Medical Sciences,
Tehran,
Iran
and
Center for Solid Waste Research, Institute for
Environmental Research,
Tehran University of Medical Sciences,
Tehran,
Iran
Waste Management Expert at Imam Khomeini
Hospital, Abadan,
Iran

Eder C. Lima
Institute of Chemistry,
Federal University of Rio Grande do Sul (UFRGS),
Av. Bento Gonçalves 9500,
Porto Alegre, RS,
Brazil

Mohammad Shirmardi
Mehdi Vosoughi
Student Research Committee,
Ahvaz Jundishapur University of Medical Sciences,
Ahvaz,
Iran

Mohammad Heidari Farsani
M.Sc. in Environmental Health Engineering, School
of Public Health,
Ahvaz Jundishapur University of Medical Sciences,
Ahvaz,
Iran

INTRODUCTION

Traditionally, the chemical compounds, which are used for eradicating or inhibiting the growth of microorganisms, are defined as antibiotics. However, the antibiotics term also includes antibacterial, antiviral, antifungal, and antitumor compounds (Homem & Santos 2011). In recent years, pharmaceutical antibiotics, due to their great therapeutic values, are widely used in human therapy against a wide variety of microorganisms to prevent infections. They were also used in livestock and farming industries as feed additive to treat diseases, improving the growth rate of animals (Zhao *et al.* 2012). The extensive and indiscriminate use of pharmaceutical antibiotics has attracted increasing concerns because they have been considered as a class of potent pollutants, which can make adverse effects such as acute and chronic toxicity. Additionally, they affect aquatic photosynthetic organisms and as a result disrupt indigenous microbial populations (Zhao *et al.* 2011a; Gao *et al.* 2012). The emergence of new strains of bacteria, which are resistant to these antibiotics, is another major concern. This in turn, may result in untreatable livestock diseases. Subsequently, possible transmission of such strains to humans may lead to untreatable human diseases (Zhang *et al.* 2011b; Gao *et al.* 2012; Babaei *et al.* 2016). Since a small portion of most antibiotics, including tetracycline (TC), could be metabolized or absorbed by the body of the treated human and animal, large fractions of these substances are excreted through urine and feces as unchanged parent compounds (Gao *et al.* 2012). Antibiotics can be released into the environment from many sources such as effluents from municipal wastewater treatment and pharmaceutical manufacturing plants because conventional water and wastewater treatment technologies cannot remove antibiotics completely (Kakavandi *et al.* 2016). The application of animals' manure and sewage sludge to agricultural fields, as fertilizers, is another major source releasing antibiotics into the environment through runoff, leaching, and other ways. Residues of these antibiotics discharged from above-mentioned sources are frequently detected in soil, surface water, groundwater, and even drinking water (Zhang *et al.* 2011b; Moussavi *et al.* 2013).

Thus, to prevent and minimize the risks related to antibiotics, effluent-containing antibiotics must be treated by an appropriate technique. Several methods have been evaluated to remove antibiotics from aqueous solutions including

conventional methods (biological process, filtration, coagulation, flocculation and sedimentation), advanced oxidation process (AOPs), membrane treatment, adsorption, and combined methods (Homem & Santos 2011; Jaafarzadeh *et al.* 2015). Each of these methods has different removal efficiency, capital costs investments, operating rates, advantages and disadvantages. Previous studies (Moussavi *et al.* 2013; Babaei *et al.* 2015; Zhang *et al.* 2015) have reported that physical-chemical methods, particularly adsorption, are appropriate and more efficient and cheaper than AOPs to remove recalcitrant and organic compounds. In adsorption process, the pollutant is removed from the aqueous effluent and transferred to a solid surface, whereas in the oxidative process, some by-products may be formed that could present a toxicity even higher than the parent pollutant (Shirmardi *et al.* 2013b; Vosoughi Niri *et al.* 2014; Yaghmaeian *et al.* 2014). The adsorption and removal of TC have been evaluated by several materials as adsorbent, including aluminum oxide (Chen & Huang 2010), montmorillonite (Zhao *et al.* 2012), kaolinite (Li *et al.* 2010), graphene oxide (Gao *et al.* 2012), soil and sediment (Zhang *et al.* 2011b), activated carbon (Choi *et al.* 2008), multi-walled carbon nanotubes (Zhang *et al.* 2011a; Babaei *et al.* 2016), and single walled carbon nanotubes (Ji *et al.* 2009). Activated carbon is an excellent adsorbent due to its porosity, large surface area, well-developed internal structure, and the presence of various functional groups on its surface. It has been extensively used for the removal of many organic and inorganic contaminants from polluted streams, which are biologically resistant (Liu *et al.* 2010; Kakavandi *et al.* 2014). In this context, there is a need to produce activated carbon from readily available materials such as agricultural by-products and wood charcoals, which can be used for industrial-scale production of activated carbons, following either physical or chemical activation (Amin 2008). In this study, activated carbon was prepared from oak charcoal, as a low-cost and abundantly available precursor in Iran, by chemical activation using $ZnCl_2$ as activating agent. Then, the performance of $ZnCl_2$ impregnated activated carbon (Zn-AC), as adsorbent, was investigated to adsorb and remove TC as a model of the most widely used antibiotics from aqueous solutions. The effects of basic variables such as pH of solution, adsorbent dosage, background electrolytes, contact time, and initial concentration on the adsorption of TC were evaluated. The kinetics and isotherms

of adsorption of TC on the prepared activated carbon were also investigated by a nonlinear fitting of the models.

MATERIALS AND METHODS

Reagents and solutions

The high-performance liquid chromatograph (HPLC) grade TC with the purity of $\geq 88\%$ was purchased from Sigma-Aldrich Chemical Co. (U.S.A) and used without further purification. The chemical structure and some main characteristics of the TC are presented in Table 1. Methanol and acetonitrile (both HPLC grade), and oxalic acid dehydrate were purchased from Merck Company, Germany. Deionized water was used throughout the experiments to prepare working solutions. All other chemicals used were analytical reagent grade and used without further purification.

Preparation and characterization of the activated carbon

Oak charcoals used as the precursor were purchased from the local natives of Lordegan County, Chaharmahal and Bakhtiari Province, Iran. To remove some ashes and impurities of the charcoals, they were washed several times with tap water; then were boiled in distilled water for 1 h, and finally were oven-dried at $110\text{ }^{\circ}\text{C}$ overnight. Afterwards, they were ground and sieved to discrete particles with the size of $\leq 300\text{ }\mu\text{m}$. Then, a 100 g of the grounded and dried char and a 50 g ZnCl_2 were added to 150 mL distilled water. The weight ratio of ZnCl_2 to precursor (char) was 0.5:1. The mixture was heated and refluxed at $100\text{ }^{\circ}\text{C}$ for 1 h under continuous magnetic stirring. The impregnated charcoals were further dried overnight in an oven at $120\text{ }^{\circ}\text{C}$, stored in a desiccator. The ZnCl_2 impregnated charcoals were transferred into a stainless steel vertical tubular reactor placed in a tube furnace and the carbonization of the pre-treated samples was carried out by ramping the temperature from $30\text{ }^{\circ}\text{C}$ to $700\text{ }^{\circ}\text{C}$ with the heating rate of $10\text{ }^{\circ}\text{C min}^{-1}$, and the samples were held at final temperature for 1 h. The reactor was continuously

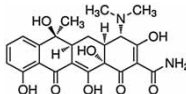
purged with a constant N_2 (99.996%) flow rate of $150\text{ cm}^3\text{ min}^{-1}$. After the samples were cooled down at $50\text{ cm}^3\text{ min}^{-1}$ of N_2 , to complete the chemical activation process, inorganics of the Zn-AC adsorbent were leached with a 6 mol L^{-1} HCl as described elsewhere (Ribas *et al.* 2014). After acidification, the obtained samples of activated carbon (Zn-AC) were thoroughly washed with hot and cold distilled water respectively until the pH of the washing solutions reached 6–7. Finally, the samples were dried at $110\text{ }^{\circ}\text{C}$ overnight in an oven, and were stored in plastic containers for subsequent uses. The same procedure has already been applied for the production of activated carbon (Ribas *et al.* 2014).

The Zn-AC was characterized using Field Emission Scanning Electron Microscope (FESEM, model Mira 3-XMU) to observe surface morphologies of the adsorbent. The elemental composition of the adsorbent was determined using a CHNS/O analyzer. The Zn-AC was also characterized by X-ray diffraction (XRD) using a PHILIPS-PW1840 X-ray diffractometer, operating at 40 kV and 30 mA with Cu $K\alpha$ radiation ($\lambda = 0.15406\text{ nm}$). Measurements were done with scanning step width of 0.02 ° and time per step of 0.4 s, over the 2θ range of $10\text{--}90\text{ }^{\circ}$. The specific surface area of the adsorbent was measured using the Brunauer, Emmett, and Teller method.

Adsorption experiments

To investigate the adsorption of TC onto the Zn-AC, batch adsorption experiments were carried out using a series of 100 mL brown volumetric flasks containing 50 mL TC solution of known concentration. This type of flask was used to prevent possible light degradation of TC. The flasks were then transferred to a thermostatic reciprocating shaker and agitated at 250 rpm at 293 K. A series adsorption experiments were performed to evaluate the effects of operational parameters such as solution pH, contact time, initial concentration of TC, adsorbent dosage, and effect of inorganic cations and anions that could interfere in the adsorption of TC. All experiments were carried out in duplicate and the average value was reported. In addition, the adsorption kinetics and isotherms were analyzed. As

Table 1 | Chemical structure and main characteristics of TC antibiotic

Name	Chemical formula	Molecular weight	Molecular structure	pK_{a1}	pK_{a2}	pK_{a3}
TC	$\text{C}_{22}\text{H}_{24}\text{N}_2\text{O}_8 \cdot x\text{H}_2\text{O}$	444.43		3.3	7.68	9.68

mentioned previously, for each working day, a fresh standard stock solution of TC was prepared by weighting and dissolving the required amounts of TC in the deionized water. The experimental solutions with different initial concentrations were obtained by diluting the stock solution in the required proportions.

Effect of solution pH

The first step in this work was to study the effect of pH on TC adsorption. To determine the optimum pH at which maximum adsorption could be achieved, the initial pH of the solutions (50 mL, initial concentration 50 and 100 mg L⁻¹) was adjusted from 3 to 11 using 0.1 M HCl or NaOH. The adsorbent dosage and the agitation time were fixed at 1 g L⁻¹ and 4 h, respectively. In addition, another set of brown flasks containing the same concentrations of TC without the adsorbent were used as blanks to investigate whether pH of the adsorbate solution would have some effects on TC adsorption.

Effect of contact time and kinetic studies

The experiments for investigating the effect of contact time and adsorption kinetics were carried out by adding 1 g L⁻¹ of the adsorbent into the initial TC concentrations of 25, 50, and 100 mg L⁻¹. The contact time ranged from 10 to 420 min, and when the predetermined time elapsed, the sample was withdrawn and filtered using a syringe membrane filter with the pore size of 0.22 μm. The filtrate was kept in a refrigerator below 4 °C before the measurement of the residual TC concentration. It is worth noting that the final pH of the adsorbate solution was close to the initial pH (4.7). For kinetics studies, nonlinear form of the pseudo-first order, pseudo-second-order, general-order kinetic models, and intra-particle diffusion models were used to evaluate the kinetic data. These models are given by Equations (1)–(4), respectively (Weber & Morris 1963; Ho 2006; Liu & Liu 2008; Cardoso *et al.* 2011b; Machado *et al.* 2012).

$$q_t = q_e \cdot [1 - \exp(-k_f \cdot t)] \quad (1)$$

$$q_t = \frac{k_s \times q_e^2 \times t}{1 + q_e \times k_s \times t} \quad (2)$$

$$q_t = q_e - \frac{q_e}{[k_N(q_e)^{n-1} \times t \times (n-1) + 1]^{1/1-n}} \quad (3)$$

$$q_t = k_{id}\sqrt{t} + C \quad (4)$$

where t is the contact time (min); q_t is the amount of adsorbate adsorbed at time t (mg g⁻¹); q_e is the amount of adsorbate adsorbed at the equilibrium (mg g⁻¹); k_f is the pseudo-first order rate constant (min⁻¹); k_s is the pseudo-second order rate constant (g mg⁻¹ min⁻¹); k_N is the general order rate constant [min⁻¹ × (g mg⁻¹)ⁿ⁻¹]; n is the order of kinetic adsorption (n could be an integral or a fractional number); k_{id} is the intra-particle diffusion rate constant (mg g⁻¹ h^{-0.5}); and C is a constant related to the thickness of boundary layer (mg g⁻¹) (Machado *et al.* 2012; dos Santos *et al.* 2014).

Equilibrium studies

To obtain the adsorption isotherms, 1 g L⁻¹ of the Zn-AC were added to TC solutions with the concentration ranging from 10 mg L⁻¹ to 250 mg L⁻¹, using a contact time of 4 h and original pH of solution (4.0–5.0). In this work, nonlinear equations of the Langmuir (Langmuir 1918), Freundlich (Freundlich 1906), Liu (Liu *et al.* 2003), and Redlich–Peterson (Redlich & Peterson 1959) isotherm models, as respectively shown in Equations (5)–(8), were used to fit the experimental data. These models are widely used to fit the adsorption of various contaminants on carbon based adsorbent such as activated carbon (Saucier *et al.* 2015a), biochars (Mohan *et al.* 2011), and CNTs (Shirmardi *et al.* 2013a).

$$q_e = \frac{Q_{\max} \times K_L \times C_e}{1 + K_L \times C_e} \quad (5)$$

$$q_e = K_F \times C_e^{1/n_F} \quad (6)$$

$$q_e = \frac{Q_{\max} \times (K_g \times C_e)^{n_L}}{1 + (K_g \times C_e)^{n_L}} \quad (7)$$

$$q_e = \frac{K_{RP} \times C_e}{1 + a_{RP} \times C_e^g} \quad \text{where } 0 < g \leq 1 \quad (8)$$

where q_e is the amount of adsorbate (TC) adsorbed at the equilibrium (mg g⁻¹); C_e is the equilibrium concentration of the adsorbate (mg L⁻¹); Q_{\max} is the maximum adsorption capacity of the adsorbent (mg g⁻¹); K_L is the Langmuir equilibrium constant (L mg⁻¹); K_F is the Freundlich equilibrium constant [mg g⁻¹ × (mg L⁻¹)^{-1/n_F}]; K_g is the Liu equilibrium

constant (L mg^{-1}); n_F and n_L are the dimensionless exponents of Freundlich and Liu models, respectively. K_{RP} and a_{RP} are Redlich–Peterson constants with the respective units of L g^{-1} and $(\text{mg L}^{-1})^{-g}$, and g is the Redlich–Peterson exponent (dimensionless) whose value should be ≤ 1 .

Effect of Zn-AC dosage

The Zn-AC at different dosages (0.25, 0.5, 0.75, 1, 1.25, 1.5, 2, 3 and 3.5 g L^{-1}) were added to the flasks containing three initial TC concentrations of 50, 75, and 100 mg L^{-1} . The other variables such as contact time and solution pH were 4 h and original pH of the solutions, respectively.

Effect of anions and cations on the adsorption

In order to study the effects of different anions and cations on the adsorption of TC, 3 g L^{-1} of the Zn-AC were added to the solutions containing 1 mM sodium salts of nitrate, bicarbonate, sulfate anions or chloride salts of cations such as potassium, magnesium, nickel (II), lithium, and iron (III) ions. In addition, the initial TC concentration and pH of the solutions were 100 mg L^{-1} and original pH, respectively. Other parameters were kept constant. One-Way ANOVA test was used to compare the results of this run.

TC determination

At the end of each run, after filtering, the residual concentration of TC in the solution was analyzed by a HPLC instrument, model Knauer with UV-VIS detector, operating at the wavelength of 360 nm. The instrument was equipped with a Eurospher column ($5 \mu\text{m } 4.6 \text{ mm} \times 250 \text{ mm}$) as well as an ultimate variable wavelength UV detection 2,500. The column temperature, the injection volume of sample, and the flow rate were 35°C , $100 \mu\text{L}$, and 1 mL min^{-1} , respectively. The mobile phase used for elution was a mixture of oxalic acid (0.01 M): methanol: acetonitrile with a volumetric ratio of 70:10:20. The residual concentration of TC in the solutions was calculated from the areas under the curves extrapolated automatically by the software. The standards of TC (initial concentration of 0.01, 0.1, 1, 5, 10, 20, 50, and 100 mg L^{-1}) were prepared and analyzed by the HPLC at operating conditions to form the calibration curve. The determination coefficient (R^2) for TC was better than 0.999. The retention time of TC was about 6.7 minutes. Similar procedure for TC determination was used elsewhere (Alavi *et al.* 2015).

The TC removal, and amount of TC adsorbed at time t ($q_t, \text{ mg g}^{-1}$) and at equilibrium ($q_e, \text{ mg g}^{-1}$) were calculated through the following equations (Equations (9)–(11)), respectively (Shirmardi *et al.* 2013a, 2013b):

$$\text{TC removal \%} = \frac{(C_o - C_e)}{C_o} \times 100 \quad (9)$$

$$q_t = \frac{(C_o - C_t) \times V}{m} \quad (10)$$

$$q_e = \frac{(C_o - C_e) \times V}{m} \quad (11)$$

where C_o and C_e (mg L^{-1}) are the initial and equilibrium concentrations of TC in the solution; m (g) is the mass of Zn-AC; V (L) is the volume of the solution; C_t (mg L^{-1}) and q_t (mg g^{-1}) are the concentration of TC at time t and the amount of TC adsorbed onto the Zn-AC at time t , respectively.

Statistical evaluation of kinetic and isotherm parameters

In this work, the kinetic and equilibrium data were fitted by employing a nonlinear method, with successive interactions calculated by the Levenberg–Marquardt method. Interactions were also calculated using the Simplex method based on the nonlinear fitting facilities of the OriginPro 2015 software. The suitability of the models was evaluated using a determination coefficient (R^2), an adjusted determination coefficient (R_{adj}^2), and a standard deviation (SD). The SD is an indication of the difference between the theoretical value of q predicted by the model and the actual q measured experimentally. The respective mathematical expressions of R^2 , R_{adj}^2 , and SD are respectively given below by Equations (12)–(14).

$$R^2 = \left(\frac{\sum_i^n (q_{i, \text{exp}} - \bar{q}_{i, \text{exp}})^2 - \sum_i^n (q_{i, \text{exp}} - q_{i, \text{model}})^2}{\sum_i^n (q_{i, \text{exp}} - \bar{q}_{i, \text{exp}})^2} \right) \quad (12)$$

$$R_{adj}^2 = 1 - (1 - R^2) \times \left(\frac{n - 1}{n - p - 1} \right) \quad (13)$$

$$SD = \sqrt{\left(\frac{1}{n - p} \right) \times \sum_i^n (q_{i, \text{exp}} - q_{i, \text{model}})^2} \quad (14)$$

in these equations, $q_{i,exp}$ represents individual value of q measured experimentally; $q_{i,model}$ represents individual value of q predicted by the fitted model; $\bar{q}_{i,exp}$ represents the average value of q measured experimentally; n is the number of experiments performed; p represents the number of parameters of the fitted model (Saucier *et al.* 2015b; Shirmardi *et al.* 2016).

RESULTS AND DISCUSSION

Characterization of the Zn-AC

The FESEM images of the prepared Zn-AC at different magnifications are shown in Figure 1. It can be seen from Figure 1 that the Zn-AC has macro-pores with different size and round shape, and the external surface of ZnCl₂ treated activated carbon (Zn-AC) is full of cavities. Although, the reason for the formation of the cavities on the

chemically activated carbon is not clear, it seems that the cavities resulted from the evaporation of ZnCl₂ used for activation during carbonization, leaving the space previously occupied by ZnCl₂ as the activating agent (Kula *et al.* 2008; Timur *et al.* 2010). Since few numbers of macro-pores are present on the outer surface of an activated carbon, the great development of macro-pores is very important, because it has been reported in the literature (Pastor-Villagas *et al.* 2006) that macro-pore structure can serve as a passage for an adsorbate to reach meso and micro-pores of the activated carbon adsorbent. The pores and cavities of the Zn-AC provide good possibility for TC to be adsorbed, as demonstrated in the next sections. The amount of C, H, N, S, and O elements in the composition of the activated carbon is presented in Table 2. The specific surface area of the Zn-AC calculated according to BET method was found to be 224 m² g⁻¹. The XRD pattern of the Zn-AC is shown in Figure 2. The characteristic peaks of activated carbon observed at $2\theta = 24^\circ$ and $2\theta = 42^\circ$ correspond to the

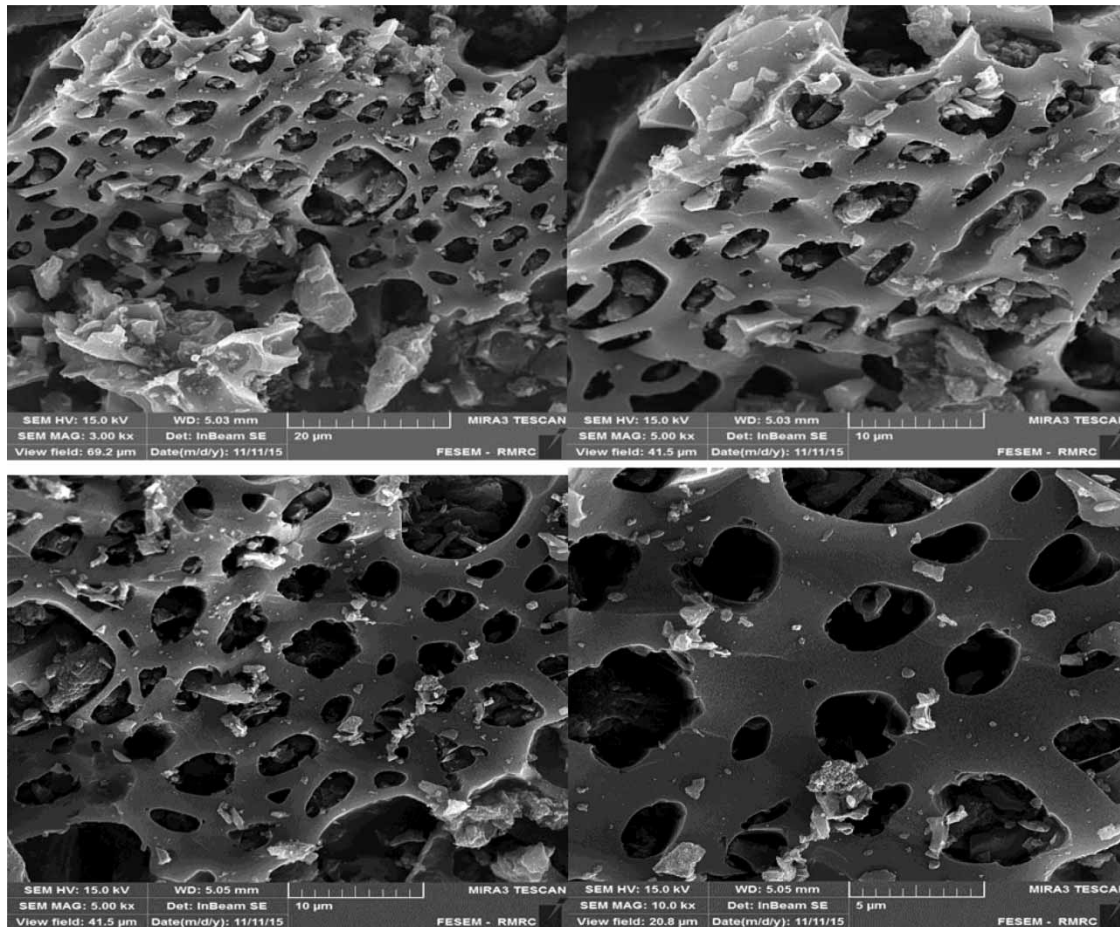
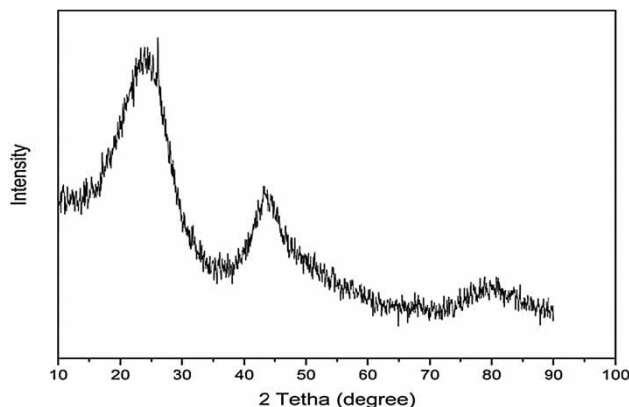


Figure 1 | FESEM images of the Zn-AC at different magnifications.

Table 2 | Quantitative results of CHNS-O analysis of the Zn-AC

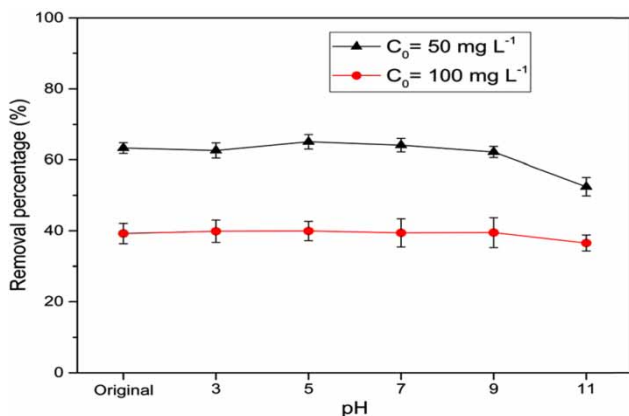
Element	C	H	N	S	O ^a
Weight (%) dry basis	87	1	0.55	–	11.45

^aBy difference.**Figure 2** | The XRD pattern of the Zn-AC.

reflections of the (002) and (100) planes, respectively, confirming that the Zn-AC activated carbon is in an amorphous state (Jache *et al.* 2012; Shang *et al.* 2015).

Effect of solution pH

It is well known that the solution pH is a very influential factor governing the adsorption because solution pH can affect the surface charge of an adsorbent as well as the speciation of an adsorbate and degree of ionization. Figure 3 shows the effect of solution pH on the adsorption of TC

**Figure 3** | Effect of pH on the adsorption of TC onto the Zn-AC. Conditions: temperature 293 K; adsorbent dosage 1 g L^{-1} . Error bars represent the SD of two replicate experiments.

onto the Zn-AC. The solution pH has no significant effect on TC adsorption onto the Zn-AC except for solution pH higher than 9. The adsorption percentage remains almost unchanged and there is no observable change in the adsorption of TC onto the Zn-AC as the solution pH is increased from 3 to 9. However, TC adsorption percentage decreases relatively considerable as the pH is increased from 9 to 11. For the initial TC concentration of 50 mg L^{-1} , the removal percentage decreases from 62% to 52% when the solution pH is increased from 3 to 11 (Figure 3). The relationship between the solution pH and TC adsorption can be related to both the surface charges and properties of the adsorbent and the pH-dependent speciation of TC antibiotic. Changing the solution pH can not only affect the protonation-deprotonation transition of functional groups on an adsorbent but also can result in a change in chemical speciation of organic compounds (Zhang *et al.* 2010, 2011a). TC (symbolized as H_2L) is an amphoteric molecule having multiple ionizable functional groups (such as amino, phenol, and alcohol), depending on the solution pH. TC has three pKa values (3.30, 7.68 and 9.68), thus it exists as cation (H_3L^+) due to the protonation of dimethyl-ammonium group when solution pH is below 3.3. At pH between 3.3 and 7.68, due to the loss of a proton from the phenolic diketone moiety, TC exists as a zwitterion (H_2L^0). At solution pH greater than 7.68, TC exists as anions (HL^- and L^{2-}) because of the loss of protons from the tri-carbonyl system and phenolic diketone moiety (Kang *et al.* 2011; Zhang *et al.* 2011a). At pH between 3.3 and 7.7, the most dominant adsorption mechanism is probably the non-electrostatic π - π dispersion interaction between bulk π systems on the Zn-AC surface and TC molecules contained both benzene rings and double bonds ($\text{C}=\text{C}$, $\text{C}=\text{O}$), or hydrophobic interaction between the Zn-AC and TC (Zhang *et al.* 2011a). In this pH range, TC exists as zwitterion, nearly all TC molecules carry no net electrical charge, and there is almost no electrostatic attraction or repulsion between TC molecules and the adsorbent. Thus, the increase of pH from 3 to 9 has no remarkable influence on the adsorption affinity of TC onto the Zn-AC. At pH above 9, the reduction in the adsorption of TC is due to the fact that with higher solution pH, the surface of the Zn-AC is negatively charged; therefore, a repulsive electrostatic interaction is established between the surface of the adsorbent and TC species (HL^- and L^{2-}), which reduces the TC adsorption (Rivera-Utrilla *et al.* 2013). It should be noted that the pH of the solutions was not fixed for the rest of our experiments since the pH of the working solutions prepared was in the range of 4–5, which TC molecules are dominantly present as zwitterion.

Kinetic studies

In the treatment of aqueous effluents by adsorption process, it is important to evaluate adsorption kinetics because some valuable pieces of information on the reaction pathways as well as on the possible mechanisms involved in the adsorption process can be obtained from adsorption kinetics (Cardoso *et al.* 2011b). The kinetic plots for the adsorption

of TC onto the Zn-AC are shown in Figure 4(a)–4(f). It is found from Figure 4 that the adsorption of TC is faster during the initial stages so that for the initial concentrations of 25 and 50 mg L⁻¹, 90% of the total removal occurs during the first 30 min of contact time. For the initial concentration of 100 mg L⁻¹, 84% of the total removal takes place during the first 30 min of the adsorption. The adsorption then becomes slow and finally reaches equilibrium at

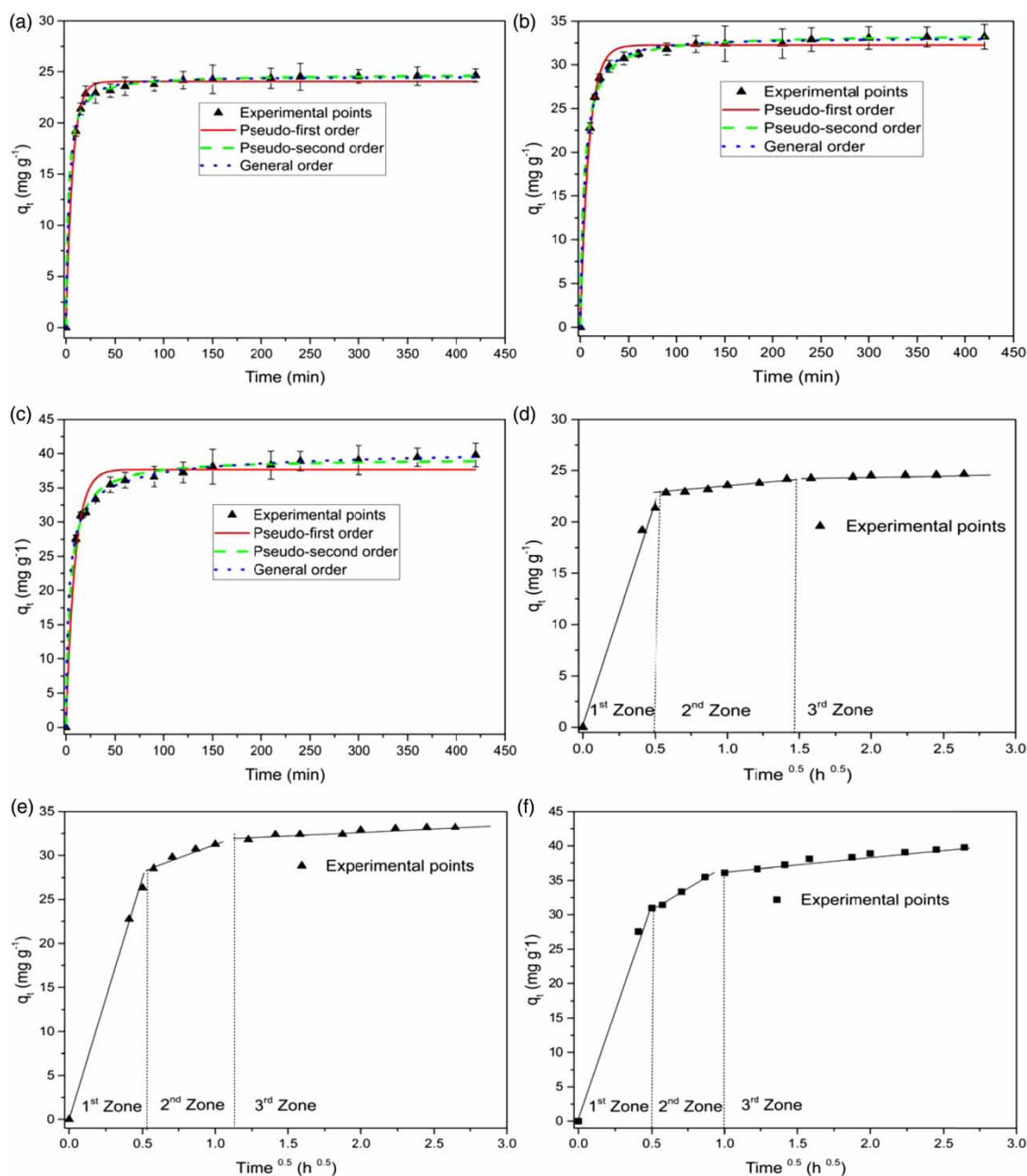


Figure 4 | Kinetic curves for the adsorption of TC onto the Zn-AC at 293 K: (a) $C_0 = 25 \text{ mg L}^{-1}$; (b) $C_0 = 50 \text{ mg L}^{-1}$; (c) $C_0 = 100 \text{ mg L}^{-1}$; (d), (e), and (f) are intra-particle diffusion model for $C_0 = 25, 50,$ and 100 mg L^{-1} , respectively. Conditions: Original pH; adsorbent dosage 1 g L^{-1} . Error bars represent the SD of two replicate experiments.

approximately 120 min for all the studied concentrations. The fitting parameters of the kinetic models are presented in Table 3. In addition to the adjusted R^2 values, the SD values were also used to explain the suitability of the fitted model since the experimental data were fitted to the non-linear kinetic models. A higher SD value is an indication showing that a higher deviation exists between q value calculated theoretically by the model and q value measured experimentally. It has been reported in the literature (Prola *et al.* 2013) that the number of parameters in nonlinear models could have influence on the fitted curves. Therefore, due to this fact, we took into consideration the number of parameters of each model (p term in Equation (13)) for calculating the SD values and evaluating the kinetic models. The minimum SD value was used to divide the SD value of each model (SD ratio); and subsequently, the SD ratio value was utilized to compare the fitness of each individual

Table 3 | Kinetic parameters obtained from the nonlinear models for the adsorption of TC onto the Zn-AC

Kinetic model	TC concentration mg L^{-1}		
	25	50	100
Pseudo-first-order			
K_f (min^{-1})	0.1521	0.1137	0.1116
q_e (mg g^{-1})	24.09	32.25	37.65
h_0 ($\text{mg g}^{-1} \text{min}^{-1}$)	3.664	3.667	4.202
SD (mg g^{-1})	0.4974	0.8158	1.706
R_{adj}^2	0.9936	0.9907	0.9705
Pseudo-second-order			
K_s ($\text{g mg}^{-1} \text{min}^{-1}$)	0.01610	0.007122	0.005620
q_e (mg g^{-1})	24.74	33.49	39.29
h_0 ($\text{mg g}^{-1} \text{min}^{-1}$)	9.849	7.991	8.674
SD (mg g^{-1})	0.3227	0.3784	0.5930
R_{adj}^2	0.9973	0.9980	0.9964
General order			
K_N [$\text{min}^{-1}(\text{g mg}^{-1})^{n-1}$]	0.02948	0.01568	3.042×10^{-4}
q_e (mg g^{-1})	24.51	33.04	41.59
n	1.728	1.719	2.918
h_0 ($\text{mg g}^{-1} \text{min}^{-1}$)	7.412	6.395	16.13
SD (mg g^{-1})	0.3171	0.3332	0.3434
R_{adj}^2	0.9974	0.9985	0.9988
Intra-particle diffusion			
k_{id} ($\text{mg g}^{-1} \text{h}^{-0.5}$) ^a	1.646	3.465	3.410
R^2	0.9962	0.9860	0.9938

^aSecond zone.

model. For the initial TC concentrations of 25, 50, and 100 mg L^{-1} , the lowest SD values were obtained for the general order kinetic model. In this work, the SD value for the pseudo-first order kinetic model varies from 0.497 to 1.70 for the evaluated concentrations. Whereas, the SD values of the pseudo-second order and general order kinetic models are in the range of 0.33 to 0.593 and 0.317 to 0.343, respectively (Table 3). For TC concentration of 25 mg L^{-1} , the SD ratio values of the pseudo-first order, pseudo-second order, and general order kinetic models are 1.57, 1.018, and 1, respectively, while the corresponding values for TC concentration of 100 mg L^{-1} are 4.97, 1.73, and 1, respectively (Table 3). The results obtained by the fitted models clearly show that the general order kinetic model better explains the adsorption of TC onto the Zn-AC because this model exhibits the lowest SD ratio values compared to the other kinetic models. Additionally, this model shows the highest R_{adj}^2 values, as well as the q_e values predicted by the general order kinetic model are relatively closer to the q_e values measured experimentally. It should be taken into account that the general order kinetic model has different orders (n) when the adsorbate concentration is changed (see Table 3); thus, it is difficult to compare the parameters of the kinetic model. Therefore, the initial sorption rate (h_0) is a useful tool to evaluate the kinetics of a given model using the following equation (Equation (15)).

$$h_0 = K_N \times q_e^n \quad (15)$$

where h_0 is the initial sorption rate ($\text{mg g}^{-1} \text{min}^{-1}$); K_N is the rate constant [$\text{min}^{-1}(\text{g mg}^{-1})^{n-1}$]; q_e is the amount of adsorbate adsorbed at equilibrium (mg g^{-1}), and n is the order of the kinetic model. It is worth noting that when $n = 2$, this equation is the same as the initial sorption rate developed by Ho & McKay (1988). The general order kinetic model provided the most confident initial sorption rates (h_0) because our experimental kinetic data were better described by this model. Based on the general order kinetic model, the order of an adsorption process should follow the same logic as in a chemical reaction, where the order of reaction is experimentally measured (Machado *et al.* 2012) instead of being confined by a given model. The intra-particle diffusion model was also used to investigate the influence of mass transfer resistance on the binding of TC to the adsorbent, Zn-AC (see Table 3 and Figure 4(d)–4(f)). Intra-particle diffusion constant (k_{id}) in terms of $\text{mg g}^{-1} \text{h}^{-0.5}$ can be obtained from the slope of the plot of q_t (the amount adsorbed at any time) versus the square root of time. The plots of q_t versus

$t^{0.5}$ are shown in Figure 4(d)–4(f) for the three initial TC concentrations. The plots have multi-linearity relationship indicating that the adsorption process involves more than one adsorption rate (Alencar *et al.* 2012). Each linear can be attributed to each stage of the adsorption process. Accordingly, the process in which TC molecules diffuse through the solution to the external surface of the adsorbent can be referred to the first linear section, which is the fastest sorption stage, can be regarded as external surface adsorption or instantaneous adsorption (Ribas *et al.* 2014). The second stage is a delayed process, and can be attributed to the intra-particle diffusion (dos Santos *et al.* 2014). The third portion is obtained after the equilibrium and describes diffusion through smaller pores (dos Santos *et al.* 2014). The kinetic studies reveal that the minimum contact time to reach the equilibrium for the adsorption of TC onto the Zn-AC is about 120 min. For the rest of our experiments, the contact time was fixed at 240 min to ensure that the equilibrium would be attained between the adsorbate even at higher concentrations and the Zn-AC adsorbent (Cardoso *et al.* 2011b).

Equilibrium studies

Adsorption isotherms describe how the adsorbate molecules distribute between the liquid phase and the solid phase when the adsorption process reaches an equilibrium state. In other words, at a constant temperature, adsorption isotherms are used to describe the relationship between the amount of adsorbate adsorbed by the adsorbent (q_e) and the adsorbate concentration remaining in the solution after the system has reached to the equilibrium state (C_e). In addition, some information about adsorption mechanism, the affinity of the adsorbate to the adsorbent, and surface properties can be obtained from the adsorption parameters of equilibrium models. In this study, the isotherms of adsorption of TC onto the Zn-AC were carried out at 293 K using the optimum experimental conditions described previously. Figure 5 shows the adsorption isotherms of TC onto the Zn-AC, and the other parameters predicted by the nonlinear adsorption models are presented in Table 4. Based on the SD values, it is clear that the Langmuir model do not describe the equilibrium data well since this model shows the highest SD value compared with the other three models. On the other hand, the Redlich–Peterson model presents the lowest SD value indicating this model provides the best fit to the experimental data; however, it should be stressed that the Freundlich and Liu models also fit the data well, but their SD values are slightly greater than

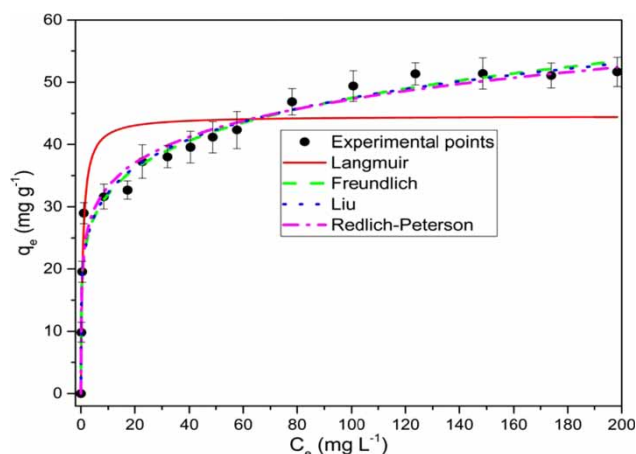


Figure 5 | Isotherm curves for the adsorption of TC onto the Zn-AC at 293 K. Conditions: original pH; adsorbent dosage 1 g L^{-1} , contact time between the adsorbent and the adsorbate 4 h. Error bars represent the SD of two replicate experiments.

Table 4 | Isotherm parameters for the adsorption of TC onto the Zn-AC adsorbent

Isotherm model	Parameter	Value
Langmuir	Q_{\max} (mg g^{-1})	44.57
	K_L (L mg^{-1})	1.411
	R_{adj}^2	0.8452
	SD (mg g^{-1})	5.946
Freundlich	K_F [$\text{mg g}^{-1} (\text{mg L}^{-1})^{-1/n}$]	21.63
	n_F	5.861
	R_{adj}^2	0.9664
	SD (mg g^{-1})	2.769
Liu	Q_{\max} (mg g^{-1})	282.1
	K_g (L mg^{-1})	2.773×10^{-6}
	n_L	0.1951
	R_{adj}^2	0.9643
Redlich–Peterson	SD (mg g^{-1})	2.855
	$K_{\text{RP}} \text{ L g}^{-1}$	284.0
	$a_{\text{RP}} (\text{mg L}^{-1})^{-g}$	11.87
	g	0.8517
	R_{adj}^2	0.9698
	SD (mg g^{-1})	2.625

the SD value of the Redlich–Peterson model (Table 4). The SD ratio was used to compare the studied isotherm models. The procedure used for calculating the SD ratio is described in the previous section (kinetic studies). The SD values of the Langmuir, Freundlich, and Liu models are 2.27, 1.06, and 1.09 times higher than the SD value obtained for the Redlich–Peterson model (Table 4). Overall, since the Redlich–Peterson model provides the highest adjusted R^2 and the lowest SD values, this model best describes the equilibrium data. The maximum amount of TC adsorbed onto

the Zn-AC (Q_{\max}) predicted by the Liu model is 282.06 mg g^{-1} indicating this adsorbent is a good adsorbent for the removal of TC from aqueous solutions.

It can be obviously seen from Figure 5 that with increasing the initial TC concentration from 10 to 250 mg L^{-1} , the amount of TC adsorbed onto the Zn-AC increases from 9.83 to 51.65 mg g^{-1} , while the removal percentage decreases from 98.3% to 20.66% .

Effect of adsorbent dosage

Adsorbent dosage is another important parameter for determination of adsorption capacity. The effect of adsorbent dosage was investigated for the initial TC concentrations of 50 , 75 , and 100 mg L^{-1} by adding various amounts (in the range of 0.25 – 3.5 g L^{-1}) of the Zn-AC to the TC solutions. Figure 6 shows the removal percentage of TC as a function of the Zn-AC dosage. The percentage of TC removal increases with increasing of adsorbent dosage for the three initial concentrations evaluated. This increase could be attributed to the increase in the adsorbent surface area, which increases the number of adsorption sites available for adsorption, as already reported in several papers (Cardoso *et al.* 2011a; Babaei *et al.* 2016; Shirmardi *et al.* 2016). On the other hand, for the three initial TC concentrations, by increasing the adsorbent dosage from 0.25 g L^{-1} to 3.5 g L^{-1} , the amount of TC adsorbed onto the Zn-AC decreases remarkably (Figure 6). This phenomenon can be explained through two aspects. First, at a fixed concentration and volume of TC, the increase of the adsorbent dosage will lead to unsaturation of adsorption

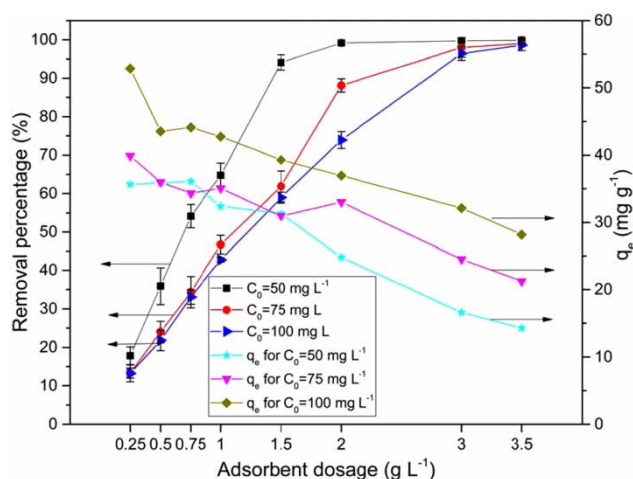


Figure 6 | Effect of the Zn-AC dosage on the adsorption of TC. Conditions: original pH; temperature 293 K ; contact time 4 h . Error bars represent the SD of two replicate experiments.

sites through the adsorption process; second, the particle aggregation, due to higher mass of the adsorbent, may result in a reduction in the adsorbent capacity. Therefore, such aggregation would lead to a decrease in the total surface area of the adsorbent and an increase in the diffusional path length (Royer *et al.* 2009). It is noteworthy that the removal percentages do not attain 100% with increasing the adsorbent dosage up to 3.5 g L^{-1} (Figure 6) confirming the particle aggregation of the adsorbent hindered complete removal of TC. In this study, since a significant increase in the removal percentage was not observed for the adsorbent quantity greater than 3 g L^{-1} for the three studied concentrations, the adsorbent dosage of 3 g L^{-1} was selected as an optimum dosage for our next experiments.

Effect of potential interferences

The effects of inorganic cations (Li^+ , K^+ , Mg^{2+} , Ca^{2+} , Ni^{2+} and Fe^{3+}) and anions (HCO_3^- , NO_3^- , and SO_4^{2-}) that could interfere in the adsorption of TC onto the Zn-AC were investigated using batch adsorption experiments, and the results are shown in Figure 7. The concentration of anions such as NO_3^- , HCO_3^- , and SO_4^{2-} and most of cations such as Li^+ , K^+ , Mg^{2+} , Ca^{2+} , Ni^{2+} and Fe^{3+} in surface water is usually less than 1 mM , as reported in the literature (Hem 1985); therefore, 1 mM salts of these anions and cations were used to evaluate their effects on TC adsorption. We used the ANOVA test to compare the adsorption of TC in the presence of the anions and cations with TC adsorption

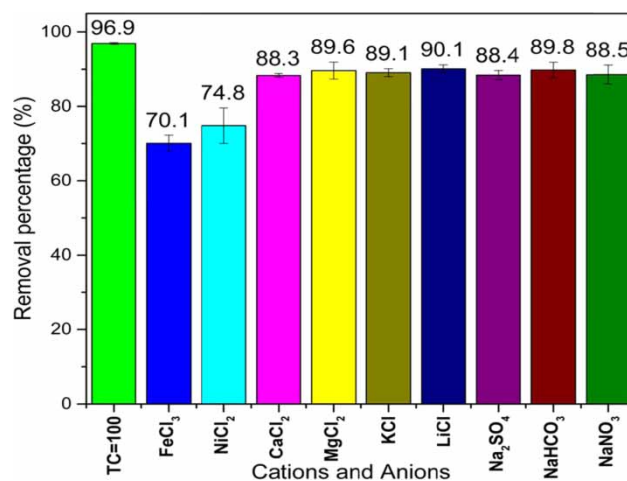


Figure 7 | The adsorption of TC onto the Zn-AC in the presence of 1 mM cations and anions, compared to the control (initial TC 100 mg L^{-1}). Conditions: original pH; temperature 293 K ; contact time 4 h ; adsorbent dosage 3 g L^{-1} . Error bars represent the SD of two replicate experiments.

in the absence of the tested anions and cations (sample containing only the adsorbent and 100 mg L⁻¹ TC). The ANOVA test results (Table 5) indicated that all tested anions and cations affected and decreased TC adsorption ($p < 0.05$). It should be noted that the presence of Fe³⁺ and Ni²⁺ decreases TC adsorption significantly; so that the removal percentage decreases from 96.9% to 70.1% for Fe³⁺ ion and from 96.9% to 74.8% for Ni²⁺ ion (Figure 7). The decrease in the adsorption of TC due to the presence of other anions and cations is less than 10% (Figure 7); the decrease in the adsorption of TC in the presence of anions and cations could be considered as a competition between the ions and TC species to adsorb on active sites of the adsorbent. The higher decrease in the adsorption of TC onto the Zn-AC due to the presence of Fe³⁺ and Ni²⁺ may be attributed to the highest tendency of Fe³⁺ and Ni²⁺ to adhere to the negatively charged Zn-AC, which in turn reduces ion interaction sites (or available sites) on the surface of the Zn-AC for TC adsorption. The results of this study are in good agreement with the results of the other researchers. For instance, Zhao *et al.* (2011b) reported that in the presence of five types of cations (Li⁺, Na⁺, K⁺, Ca²⁺, and Mg²⁺) the adsorption of TC on kaolinite decreased in accordance with the increasing of atomic radius and valence of metal cations. They attributed the decrease in the adsorption to outer-sphere complexes formed between TC and kaolinite as well as the existence of competitor ions. Liu *et al.* (2012) investigated the removal of TC from water by Fe-Mn binary oxide reported that the presence of cations and anions such as Ca²⁺, Mg²⁺, CO₃²⁻ and SO₄²⁻ had no significant effect on the TC removal in their experimental conditions, while SiO₃²⁻ and PO₄³⁻ hindered the adsorption of TC. Zhao *et al.* (2011a) evaluated the adsorption of TC onto goethite in the presence of metal cations and humic substances. They stated that at the studied pH range, the presence of five background

electrolyte cations (Li⁺, Na⁺, K⁺, Ca²⁺, and Mg²⁺) with a concentration of 0.01 M had little effect on the TC adsorption. The adsorption of four pharmaceuticals (carbamazepine, diclofenac, ibuprofen, and ketoprofen) to silica as a function of ionic strength, anions, cations, and natural organic matter was investigated by Bui & Choi (2010). The authors reported that the tested anions did not significantly affect the adsorption of these pharmaceuticals to silica ($p > 0.05$). Their results also showed that the divalent cations did not significantly affect the adsorption of carbamazepine and diclofenac; however, divalent cations at low concentrations (1 mM) increased the adsorption of ibuprofen and ketoprofen. In contrast with the present study, in that study, the presence of Fe³⁺ significantly increased the adsorption of the pharmaceuticals, but in our study, it significantly decreased the adsorption of TC. This difference may be ascribed to different structure of both adsorbate and adsorbent used in the studies. Blank experiments were also run for each anions and cations at the same conditions to observe the changes in the initial concentration of TC because of possible reactions between TC and the tested anions and cations. The change in TC concentration in the blank samples was less than 2% for all cations and anions.

CONCLUSIONS

The adsorption of TC antibiotic onto the Zn-AC as a low cost adsorbent was carried out by using a batch adsorption technique. The effects of different operational parameters such as pH of solution, adsorbent dosage, interferences cations and anions, contact time, and initial TC concentration were evaluated. The solution pH in the range of 3–9 had no considerable effect on TC adsorption. The adsorption of TC onto the adsorbent was relatively fast and reached the equilibrium after about 120 min. The results of ANOVA test showed that all the studied cations and anions affected and decreased the adsorption of TC onto the Zn-AC; however, this decrease in the removal percentage was strongly significant in the presence of Fe³⁺ and Ni²⁺ ions. The experimental data were fitted to three non-linear kinetic models, and the general order kinetic model best described the kinetic of TC adsorption. Equilibrium data were fitted to four known isotherm models, and the Redlich–Peterson model gave the best fit. The results of the present study indicate that Zn-AC can be a good alternative low cost adsorbent for the removal of TC and other pollutants from aqueous solutions.

Table 5 | Significant impact of cations and anions on the adsorption of TC onto Zn-AC

Control	Background electrolyte	Significant impact on adsorption
TC = 100 mg L ⁻¹	FeCl ₃	Yes
	NiCl ₂	Yes
	CaCl ₂	Yes
	MgCl ₂	Yes
	KCl	Yes
	LiCl	Yes
	Na ₂ SO ₄	Yes
	NaHCO ₃	Yes
	NaNO ₃	Yes

ACKNOWLEDGEMENTS

The authors are grateful to the Vice Chancellery for Research Development and Technology as well as the Environmental Technologies Research Center (ETRC) of Ahvaz Jundishapur University of Medical Sciences for funding and providing necessary facilities to accomplish this research with project number of ETRC-9307; in addition, the authors are also grateful to the National Council for Scientific and Technological Development (CNPq, Brazil).

REFERENCES

- Alavi, N., Babaei, A., Shirmardi, M., Naimabadi, A. & Goudarzi, G. 2015 Assessment of oxytetracycline and tetracycline antibiotics in manure samples in different cities of Khuzestan Province, Iran. *Environmental Science and Pollution Research* **22** (22), 17948–17954.
- Alencar, W. S., Lima, E. C., Royer, B., dos Santos, B. D., Calvete, T., da Silva, E. A. & Alves, C. N. 2012 Application of aqai stalks as biosorbents for the removal of the dye procion blue MX-R from aqueous solution. *Separation Science and Technology* **47** (3), 513–526.
- Amin, N. K. 2008 Removal of reactive dye from aqueous solutions by adsorption onto activated carbons prepared from sugarcane bagasse pith. *Desalination* **223** (1–3), 152–161.
- Babaei, A. A., Azari, A., Kalantary, R. R. & Kakavandi, B. 2015 Enhanced removal of nitrate from water using nZVI@MWCNTs composite: synthesis, kinetics and mechanism of reduction. *Water Science & Technology* **72** (11), 1988–1999.
- Babaei, A. A., Lima, E. C., Takdastan, A., Alavi, N., Goudarzi, G., Vosoughi, M., Hassani, G. & Shirmardi, M. 2016 Removal of tetracycline antibiotic from contaminated water media by multi-walled carbon nanotubes: operational variables, kinetics, and equilibrium studies. *Water Science and Technology* (in press), doi:10.2166/wst.2016.2301.
- Bui, T. X. & Choi, H. 2010 Influence of ionic strength, anions, cations, and natural organic matter on the adsorption of pharmaceuticals to silica. *Chemosphere* **80** (7), 681–686.
- Cardoso, N. F., Lima, E. C., Pinto, I. S., Amavisca, C. V., Royer, B., Pinto, R. B., Alencar, W. S. & Pereira, S. F. P. 2011a Application of cupuassu shell as biosorbent for the removal of textile dyes from aqueous solution. *Journal of Environmental Management* **92** (4), 1237–1247.
- Cardoso, N. F., Pinto, R. B., Lima, E. C., Calvete, T., Amavisca, C. V., Royer, B., Cunha, M. L., Fernandes, T. H. M. & Pinto, I. S. 2011b Removal of remazol black B textile dye from aqueous solution by adsorption. *Desalination* **269** (1–3), 92–103.
- Chen, W.-R. & Huang, C.-H. 2010 Adsorption and transformation of tetracycline antibiotics with aluminum oxide. *Chemosphere* **79** (8), 779–785.
- Choi, K.-J., Kim, S.-G. & Kim, S.-H. 2008 Removal of antibiotics by coagulation and granular activated carbon filtration. *Journal of Hazardous Materials* **151** (1), 38–43.
- dos Santos, D., Adebayo, M., de Fátima Pinheiro Pereira, S., Prola, L., Cataluña, R., Lima, E., Saucier, C., Gally, C. & Machado, F. 2014 New carbon composite adsorbents for the removal of textile dyes from aqueous solutions: kinetic, equilibrium, and thermodynamic studies. *Korean Journal of Chemical Engineering* **31** (8), 1470–1479.
- Freundlich, H. 1906 Adsorption in solution. *Phys. Chem. Soc.* **40**, 1361–1368.
- Gao, Y., Li, Y., Zhang, L., Huang, H., Hu, J., Shah, S. M. & Su, X. 2012 Adsorption and removal of tetracycline antibiotics from aqueous solution by graphene oxide. *Journal of Colloid and Interface Science* **368** (1), 540–546.
- Hem, J. D. 1985 *Study and Interpretation of the Chemical Characteristics of Natural Water*. Department of the Interior, US Geological Survey.
- Ho, Y.-S. 2006 Review of second-order models for adsorption systems. *Journal of Hazardous Materials* **136** (3), 681–689.
- Ho, Y. S. & McKay, G. 1988 Sorption of dye from aqueous solution by peat. *Chemical Engineering Journal* **70**, 115–124.
- Homem, V. & Santos, L. 2011 Degradation and removal methods of antibiotics from aqueous matrices—a review. *Journal of Environmental Management* **92** (10), 2304–2347.
- Jaafarzadeh, N., Kakavandi, B., Takdastan, A., Kalantary, R. R., Azizi, M. & Jorfi, S. 2015 Powder activated carbon/Fe₃O₄ hybrid composite as a highly efficient heterogeneous catalyst for Fenton oxidation of tetracycline: degradation mechanism and kinetic. *RSC Advances* **5** (103), 84718–84728.
- Jache, B., Neumann, C., Becker, J., Smarsly, B. M. & Adelhelm, P. 2012 Towards commercial products by nanocasting: characterization and lithium insertion properties of carbons with a macroporous, interconnected pore structure. *Journal of Materials Chemistry* **22** (21), 10787–10794.
- Ji, L., Chen, W., Duan, L. & Zhu, D. 2009 Mechanisms for strong adsorption of tetracycline to carbon nanotubes: a comparative study using activated carbon and graphite as adsorbents. *Environmental Science & Technology* **43** (7), 2322–2327.
- Kakavandi, B., Esrafil, A., Mohseni-Bandpi, A., Jonidi Jafari, A. & Rezaei Kalantary, R. 2014 Magnetic Fe₃O₄@C nanoparticles as adsorbents for removal of amoxicillin from aqueous solution. *Water Science & Technology* **69** (1), 147–155.
- Kakavandi, B., Takdastan, A., Jaafarzadeh, N., Azizi, M., Mirzaei, A. & Azari, A. 2016 Application of Fe₃O₄@C catalyzing heterogeneous UV-Fenton system for tetracycline removal with a focus on optimization by a response surface method. *Journal of Photochemistry and Photobiology A: Chemistry* **314**, 178–188.
- Kang, J., Liu, H., Zheng, Y.-M., Qu, J. & Chen, J. P. 2011 Application of nuclear magnetic resonance spectroscopy, Fourier transform infrared spectroscopy, UV-Visible spectroscopy and kinetic modeling for elucidation of adsorption chemistry in uptake of tetracycline by zeolite beta. *Journal of Colloid and Interface Science* **354** (1), 261–267.
- Kula, I., Uğurlu, M., Karaoğlu, H. & Çelik, A. 2008 Adsorption of Cd(II) ions from aqueous solutions using activated carbon prepared from olive stone by ZnCl₂ activation. *Bioresource Technology* **99** (3), 492–501.

- Langmuir, I. 1918 The adsorption of gases on plane surfaces of glass, mica and platinum. *Journal of the American Chemical Society* **40** (9), 1361–1403.
- Li, Z., Schulz, L., Ackley, C. & Fenske, N. 2010 Adsorption of tetracycline on kaolinite with pH-dependent surface charges. *Journal of Colloid and Interface Science* **351** (1), 254–260.
- Liu, Y. & Liu, Y.-J. 2008 Biosorption isotherms, kinetics and thermodynamics. *Separation and Purification Technology* **61** (3), 229–242.
- Liu, Y., Xu, H., Yang, S.-F. & Tay, J.-H. 2003 A general model for biosorption of Cd^{2+} , Cu^{2+} and Zn^{2+} by aerobic granules. *Journal of Biotechnology* **102** (3), 233–239.
- Liu, Q.-S., Zheng, T., Wang, P. & Guo, L. 2010 Preparation and characterization of activated carbon from bamboo by microwave-induced phosphoric acid activation. *Industrial Crops and Products* **31** (2), 233–238.
- Liu, H., Yang, Y., Kang, J., Fan, M. & Qu, J. 2012 Removal of tetracycline from water by Fe-Mn binary oxide. *Journal of Environmental Sciences* **24** (2), 242–247.
- Machado, F. M., Bergmann, C. P., Lima, E. C., Royer, B., de Souza, F. E., Jauris, I. M., Calvete, T. & Fagan, S. B. 2012 Adsorption of Reactive Blue 4 dye from water solutions by carbon nanotubes: experiment and theory. *Physical Chemistry Chemical Physics* **14** (31), 11139–11153.
- Mohan, D., Rajput, S., Singh, V. K., Steele, P. H. & Pittman, Jr. C. U. 2011 Modeling and evaluation of chromium remediation from water using low cost bio-char, a green adsorbent. *Journal of Hazardous Materials* **188** (1–3), 319–333.
- Moussavi, G., Alahabadi, A., Yaghmaeian, K. & Eskandari, M. 2013 Preparation, characterization and adsorption potential of the NH_4Cl -induced activated carbon for the removal of amoxicillin antibiotic from water. *Chemical Engineering Journal* **217**, 119–128.
- Pastor-Villegas, J., Pastor-Valle, J. F., Rodríguez, J. M. M. & García, M. G. 2006 Study of commercial wood charcoals for the preparation of carbon adsorbents. *Journal of Analytical and Applied Pyrolysis* **76** (1–2), 103–108.
- Prola, L. D. T., Machado, F. M., Bergmann, C. P., de Souza, F. E., Gally, C. R., Lima, E. C., Adebayo, M. A., Dias, S. L. P. & Calvete, T. 2013 Adsorption of Direct Blue 53 dye from aqueous solutions by multi-walled carbon nanotubes and activated carbon. *Journal of Environmental Management* **130** (0), 166–175.
- Redlich, O. & Peterson, D. L. 1959 A useful adsorption isotherm. *Journal of Physical Chemistry* **63** (6), 1024–1024.
- Ribas, M. C., Adebayo, M. A., Prola, L. D. T., Lima, E. C., Cataluña, R., Feris, L. A., Puchana-Rosero, M. J., Machado, F. M., Pavan, F. A. & Calvete, T. 2014 Comparison of a homemade cocoa shell activated carbon with commercial activated carbon for the removal of reactive violet 5 dye from aqueous solutions. *Chemical Engineering Journal* **248**, 315–326.
- Rivera-Utrilla, J., Gómez-Pacheco, C. V., Sánchez-Polo, M., López-Peñalver, J. J. & Ocampo-Pérez, R. 2013 Tetracycline removal from water by adsorption/bioadsorption on activated carbons and sludge-derived adsorbents. *Journal of Environmental Management* **131**, 16–24.
- Royer, B., Cardoso, N. F., Lima, E. C., Ruiz, V. S. O., Macedo, T. R. & Airoldi, C. 2009 Organofunctionalized kenyaite for dye removal from aqueous solution. *Journal of Colloid and Interface Science* **336** (2), 398–405.
- Saucier, C., Adebayo, M. A., Lima, E. C., Cataluña, R., Thue, P. S., Prola, L. D., Puchana-Rosero, M. J., Machado, F. M., Pavan, F. A. & Dotto, G. L. 2015a Microwave-assisted activated carbon from cocoa shell as adsorbent for removal of sodium diclofenac and nimesulide from aqueous effluents. *Journal of Hazardous Materials* **289**, 18–27.
- Saucier, C., Adebayo, M. A., Lima, E. C., Prola, L. D. T., Thue, P. S., Umpierrez, C. S., Rosero, M. J. P. & Machado, F. M. 2015b Comparison of a homemade bacuri shell activated carbon with carbon nanotubes for food dye removal. *CLEAN – Soil, Air, Water* **43**, 1389–1400.
- Shang, H., Lu, Y., Zhao, F., Chao, C., Zhang, B. & Zhang, H. 2015 Preparing high surface area porous carbon from biomass by carbonization in a molten salt medium. *RSC Advances* **5** (92), 75728–75734.
- Shirmardi, M., Mahvi, A., Hashemzadeh, B., Naeimabadi, A., Hassani, G. & Niri, M. 2013a The adsorption of malachite green (MG) as a cationic dye onto functionalized multi walled carbon nanotubes. *Korean Journal of Chemical Engineering* **30** (8), 1603–1608.
- Shirmardi, M., Mahvi, A. H., Mesdaghinia, A., Nasser, S. & Nabizadeh, R. 2013b Adsorption of acid red18 dye from aqueous solution using single-wall carbon nanotubes: kinetic and equilibrium. *Desalination and Water Treatment* **51** (34–36), 6507–6516.
- Shirmardi, M., Alavi, N., Lima, E. C., Takdastan, A., Mahvi, A. H. & Babaei, A. A. 2016 Removal of atrazine as an organic micro-pollutant from aqueous solutions: a comparative study. *Process Safety and Environmental Protection* **103**, 23–35.
- Timur, S., Kantarli, I. C., Onenc, S. & Yanik, J. 2010 Characterization and application of activated carbon produced from oak cups pulp. *Journal of Analytical and Applied Pyrolysis* **89** (1), 129–136.
- Vosoughi Niri, M., Shirmardi, M., Asadi, A., Golestani, H., Naeimabadi, A., Mohammadi, M. J. & Heidari Farsani, M. 2014 Reactive red 120 dye removal from aqueous solution by adsorption on nano-alumina. *Journal of Water Chemistry and Technology* **36** (3), 125–133.
- Weber, W. J. & Morris, J. C. 1963 Kinetics of adsorption on carbon from solution. *Journal of the Sanitary Engineering Division* **89** (2), 31–60.
- Yaghmaeian, K., Moussavi, G. & Alahabadi, A. 2014 Removal of amoxicillin from contaminated water using NH_4Cl -activated carbon: continuous flow fixed-bed adsorption and catalytic ozonation regeneration. *Chemical Engineering Journal* **236**, 538–544.
- Zhang, S., Shao, T., Bekaroglu, S. S. K. & Karanfil, T. 2010 Adsorption of synthetic organic chemicals by carbon nanotubes: effects of background solution chemistry. *Water Research* **44** (6), 2067–2074.

- Zhang, L., Song, X., Liu, X., Yang, L., Pan, F. & Lv, J. 2011a Studies on the removal of tetracycline by multi-walled carbon nanotubes. *Chemical Engineering Journal* **178**, 26–33.
- Zhang, Z., Sun, K., Gao, B., Zhang, G., Liu, X. & Zhao, Y. 2011b Adsorption of tetracycline on soil and sediment: effects of pH and the presence of Cu(II). *Journal of Hazardous Materials* **190** (1–3), 856–862.
- Zhang, D., Yin, J., Zhao, J., Zhu, H. & Wang, C. 2015 Adsorption and removal of tetracycline from water by petroleum coke-derived highly porous activated carbon. *Journal of Environmental Chemical Engineering* **3** (3), 1504–1512.
- Zhao, Y., Geng, J., Wang, X., Gu, X. & Gao, S. 2011a Adsorption of tetracycline onto goethite in the presence of metal cations and humic substances. *Journal of Colloid and Interface Science* **361** (1), 247–251.
- Zhao, Y., Geng, J., Wang, X., Gu, X. & Gao, S. 2011b Tetracycline adsorption on kaolinite: pH, metal cations and humic acid effects. *Ecotoxicology* **20** (5), 1141–1147.
- Zhao, Y., Gu, X., Gao, S., Geng, J. & Wang, X. 2012 Adsorption of tetracycline (TC) onto montmorillonite: cations and humic acid effects. *Geoderma* **183–184**, 12–18.

First received 4 April 2016; accepted in revised form 11 August 2016. Available online 3 September 2016